AGU PUBLICATIONS

Tectonics

RESEARCH ARTICLE
10.1002/2013TC003511

Key Points:
- New $^{40}Ar/^{39}Ar$ data update the age of the Cretaceous magmatism in NE Iberia
- Magmatism in the Pyrenees postdates the rotation of Iberia
- Magmatism in the Catalonian Coastal Ranges could mark the onset of Alpine shortening

Supporting Information:
- Readme
- Appendix S1
- Tables S1–S9

Correspondence to:
T. Ubide,
teresaubide@gmail.com

Citation:
Ubide, T., J. R. Wijbrans, C. Galé, E. Arranz, M. Lago, and P. Larrea (2014), Age of the Cretaceous alkaline magmatism in northeast Iberia: Implications for the Alpine cycle in the Pyrenees, *Tectonics*, *33*, 1444–1460, doi:10.1002/2013TC003511.

Received 17 DEC 2013
Accepted 7 JUL 2014
Accepted article online 16 JUL 2014
Published online 29 JUL 2014

Age of the Cretaceous alkaline magmatism in northeast Iberia: Implications for the Alpine cycle in the Pyrenees

Teresa Ubide[1,2], Jan R. Wijbrans[1], Carlos Galé[2], Enrique Arranz[2], Marceliano Lago[2], and Patricia Larrea[2]

[1]Department of Earth Sciences, Faculty of Earth and Life Sciences, VU University Amsterdam, Amsterdam, Netherlands, [2]Department of Earth Sciences, Faculty of Sciences, Universidad de Zaragoza, Zaragoza, Spain

Abstract Cretaceous magmatism in northeast Iberia is related to the opening of the Bay of Biscay and counterclockwise rotation of Iberia with respect to Europe and predates the collision between Iberia and Europe that resulted in the formation of the Pyrenees. To better constrain the age of this magmatism, we have undertaken a $^{40}Ar/^{39}Ar$ study on samples from the Pyrenees and the Catalonian Coastal Ranges. In the Basque-Cantabrian Basin and the North Pyrenean Basins, we have obtained Albian ages (ca. 102 Ma). In the northern Catalonian Coastal Ranges, we have obtained Campanian ages (ca. 79 Ma). We integrate our data with a review of previously published ages and discuss our results in terms of their geodynamic significance. The Cretaceous magmatism in the Pyrenees is Albian-Santonian (mostly occurring between 105 to 85 Ma) and was emplaced in a tectonically unclear context after the opening of the Bay of Biscay and rotation of Iberia. The magmatism in the Catalonian Coastal Ranges is well constrained to ca. 79 Ma and could mark the onset of Alpine shortening in the Pyrenean realm in northeasternmost Iberia. Finally, we describe a Late Triassic (ca. 232 Ma)–Early Jurassic (ca. 180 Ma) phase of magmatism in the Central Pyrenees, previously considered to be Cretaceous, that widens temporally and geographically the extent of the rift-related alkaline magmatism in southwestern Europe at that time.

1. Introduction

During the Cretaceous, the northeast of Iberia underwent an important geodynamic event linked to ocean-floor spreading in the North Atlantic: the V-shaped Bay of Biscay opened, leading to ca. 35° of counterclockwise rotation and consequent separation of Iberia with respect to Europe [*Bullard et al*., 1965; *Carey*, 1958; *Choukroune*, 1992; *Gong et al*., 2008; *Sibuet et al*., 2004; *Van der Voo*, 1969]. This event has attracted considerable interest: the debate is fuelled by the fact that the main rotation of Iberia occurred between magnetic anomalies M0 and A34 (base of the Aptian and Santonian, respectively, according to the recent geologic timescale by *Walker and Geissman* [2009]) during the Cretaceous Normal Superchron, and hence, no reliable sea-floor magnetic anomalies exist to document the intermediate stages of the process [e.g., *Vissers and Meijer*, 2012a]. Furthermore, there is a discrepancy between plate-kinematic models and the geological record in the Pyrenees, so the kinematics of opening of the Bay of Biscay and related Iberia rotation remains controversial [e.g., *Jammes et al*., 2009; *Vissers and Meijer*, 2012a].

In a recent interpretation, the entire rotation of Iberia has been confined to the Aptian period [*Gong et al*., 2008], and *Vissers and Meijer* [2012a] have proposed that a stagnant tectonic stage took place between the end of rotation and the beginning of Alpine collision between Iberia and Europe in the Late Cretaceous. Compression continued during the Tertiary, eventually leading to the formation of the Pyrenean chain. The exact age for the onset of shortening is, however, not clear. Plate-kinematic reconstructions by *Rosenbaum et al*. [2002] fix the onset of Iberia-Europe convergence right at the end of the Cretaceous Normal Superchron (magnetic anomaly A34, Santonian according to *Walker and Geissman* [2009]). On the other hand, different geological studies in the Pyrenees report slightly different ages from the Santonian to the Maastrichtian for the onset of compression [e.g., *Beaumont et al*., 2000; *Garrido-Megías and Ríos-Aragüés*, 1972; *Muñoz*, 1992; *Puigdefàbregas and Souquet*, 1986]. More recently, *Vissers and Meijer* [2012a, 2012b] stress that there is no geological evidence in the Pyrenees for any significant crustal shortening prior to the Campanian.

In this geodynamic scenario, magmatic activity developed at the transition between the Iberian and European domains and is recorded today in the northeast part of the Iberian Peninsula. This magmatism crops out in several zones along the Pyrenees and as isolated intrusions in the northern part of the Catalonian Coastal Ranges. Because of its Cretaceous age and alkaline geochemical affinity, it belongs to the Late Cretaceous Alkaline Igneous Province in the Iberian Peninsula defined by *Rock* [1982] and it could also be ascribed to the Cretaceous Peri-Atlantic Alkaline Pulse defined by *Matton and Jébrak* [2009]. The Cretaceous magmatism in northeast Iberia has traditionally been related to the opening of the Bay of Biscay and allied rotation of Iberia [e.g., *Montigny et al*., 1986; *Rock*, 1982] and to the period between the end of rotation and the beginning of Iberia-Europe collision [*Solé et al*., 2003; *Vissers and Meijer*, 2012a]. It follows that the age of the magmatism potentially gives insights on the discussed geodynamic evolution of the Iberia-Europe plate boundary during the Alpine cycle. Following this approach, *Montigny et al*. [1986] carried out a wide geochronological study on the Cretaceous magmatism and LP/HT metamorphism in the Pyrenees, concluding that magmatic activity took place between 110 and 85 Ma (Albian and Santonian, respectively, according to the recent geologic timescale by *Walker and Geissman* [2009]); despite being the most complete isotopic study carried out to date, it was published more than 20 years ago and used the conventional $^{40}K/^{40}Ar$ dating method, yielding results with relatively high uncertainties. Further isotopic dating has only been carried out in the eastern part of the Pyrenees [*Golberg et al*., 1986; *Vitrac-Michard et al*., 1977] and in the Catalonian Coastal Ranges [*Solé et al*., 2003] and yielded rather varying results.

The primary aim of the present study is to better constrain the age of the Cretaceous magmatism in northeast Iberia, in the light of new $^{40}Ar/^{39}Ar$ ages. We have dated samples from the Pyrenees and the Catalonian Coastal Ranges, most of which belong to newly studied outcrops. Additionally for certain samples, we have dated both macrocryst and groundmass separates to double check the results. The new ages, together with a careful evaluation of previous data, allow us to present a detailed geochronology for the Cretaceous magmatism in northeast Iberia. This will be used to shed some light on the long-standing debate regarding the geodynamic evolution of the area during the Alpine cycle, including the kinematics of opening of the Bay of Biscay and associated Iberia rotation, as well as the age of onset of Pyrenean shortening.

2. The Cretaceous Magmatism in Northeast Iberia: Geological Context, Characterization, and Previous Dating Results

2.1. Pyrenees

The Pyrenees belong to the long Alpine-Himalayan Tertiary collision system and formed in response to convergent motions between Iberia and Eurasia [e.g., *Muñoz*, 1992; *Vergés et al*., 2002]. The Pyrenees constitute an E-W trending, bivergent mountain chain divided into several zones (Figure 1) [e.g., *Choukroune*, 1992]. Due to postorogenic erosion and exhumation [*Fitzgerald et al*., 1999], the Paleozoic basement crops out in the central area of the chain, in the Pyrenean Axial Zone. To the north of the Axial Zone, mainly Mesozoic uplifted sedimentary basins make up the narrow North Pyrenean Zone. To the south, Mesozoic and Tertiary sediments make up the South Pyrenean Zone. Finally, Tertiary foreland deposits compose the Aquitanian and Ebro basins. The North Pyrenean Fault Zone, roughly parallel to the trend of the Pyrenees and located between the North Pyrenean Zone and the Axial Zone (Figure 1), separates the Iberian and European domains [*Vissers and Meijer*, 2012a, 2012b, and references therein].

Cretaceous magmatism crops out in several zones along the Pyrenees (Figure 1), namely, the Basque-Cantabrian Basin (Bilbao-San Sebastián area in the Western Pyrenees), the North Pyrenean Basins (Pau-Tarbes area and Saint-Gaudens oil drillings), and the Eastern Pyrenees (Corbières-Fitou area, between Narbonne and Perpignan). The magmatism is alkaline in composition [*Azambre et al*., 1992; *Cabanis and Le Fur-Balouet*, 1990, and references therein] and was emplaced into Mesozoic sediments of the North Pyrenean Zone, to the north of the North Pyrenean Fault Zone, thus within the European domain. In the Basque-Cantabrian Basin, the Cretaceous magmatism is widespread and comprises a great variety of rock types including acid and basic volcanic, volcaniclastic, and intrusive rocks; extrusive rocks are the most common and reach more than 1000 m in thickness [e.g., *Carracedo-Sánchez et al*., 2012]. Toward the east, magmatic occurrences are progressively scarcer, and no extrusive rocks are known in the Eastern Pyrenees, where lamprophyre dikes, small nepheline-syenite stocks, and amphibole gabbros represent the Cretaceous igneous rocks. The magmatism in the Eastern Pyrenees is silica undersaturated, in contrast with its saturated character in the rest

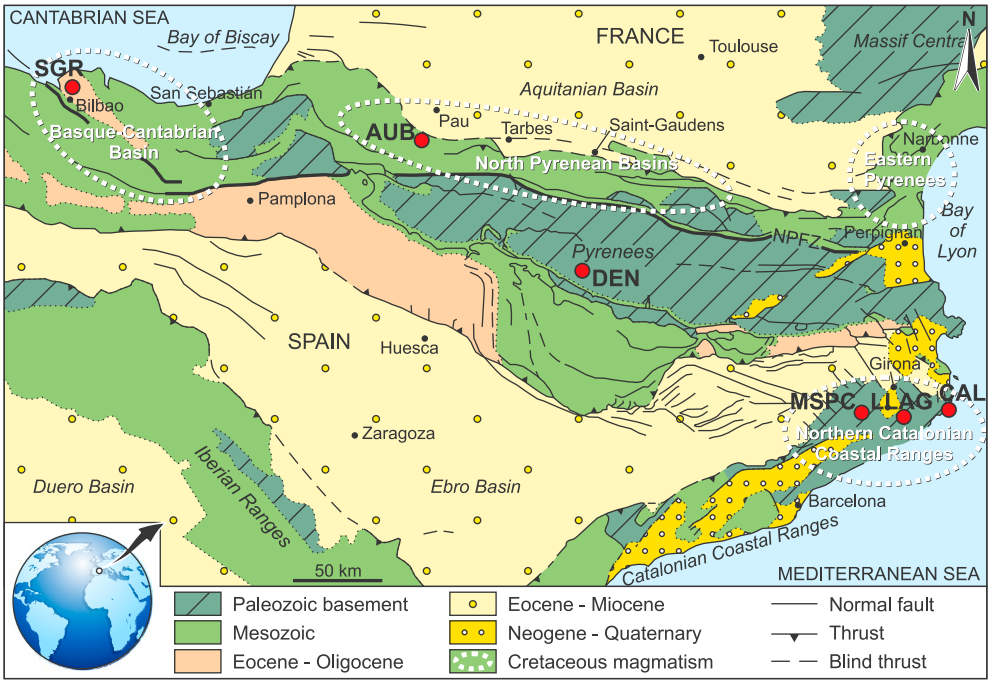

Figure 1. Location and geological map of northeast Iberia (modified from *Vergés et al.* [2002]) indicating the domains where the Cretaceous magmatism crops out. From west to east: Basque-Cantabrian Basin, North Pyrenean Basins, Eastern Pyrenees, and Catalonian Coastal Ranges. Cretaceous igneous rocks are progressively more intrusive and silica undersaturated toward the east. Red circles indicate the location of the studied outcrops. SGR: Sangroniz; AUB: L'Aubisqué; DEN: Denuy; CAL: Calella de Palafrugell; LLAG: Llagostera; MSPC: Monasterio de Sant Pere Cercada. NPFZ: North Pyrenean Fault Zone (thick black line).

of the chain [*Azambre et al.*, 1992; *Cabanis and Le Fur-Balouet*, 1990]. These variations along the Pyrenees have been interpreted in terms of contrasting geotectonic evolution and differences in melting rate [*Azambre et al.*, 1992; *Cabanis and Le Fur-Balouet*, 1990] of an initially similar, enriched mantle source situated beneath the lithosphere [*Rossy et al.*, 1992].

In the Basque-Cantabrian Basin, the oldest Cretaceous extrusive rocks are interbedded with sediments of the Early Albian [*Fernández-Mendiola and García-Mondéjar*, 2003, and references therein]. In the interval from the Late Albian to the Santonian, several extrusive stages are recognized [*Castañares and Robles*, 2004, and references therein]. The ^{40}K/^{40}Ar ages obtained from the intrusive rocks in this domain range between ca. 104 and 84 Ma [*Montigny et al.*, 1986]. In the North Pyrenean Basins, extrusive rocks are dated at the Albian-Cenomanian boundary in the Pau-Tarbes area [*Schoeffler et al.*, 1964] and have also been recognized at the Saint-Gaudens boreholes covering the Late Albian–Turonian period. Intrusive rocks cover a wide variation range between ca. 110 and 90 Ma (^{40}K/^{40}Ar ages: *Montigny et al.* [1986]). Finally, isotopic ages of the intrusive rocks in the Eastern Pyrenees range between ca. 95 and 82 Ma (^{40}Ar/^{39}Ar: *Golberg et al.* [1986]; ^{40}K/^{40}Ar: *Montigny et al.* [1986]; ^{87}Rb/^{86}Sr and ^{40}Ar/^{39}Ar: *Vitrac-Michard et al.* [1977]).

In addition to these outcrops, *Mey* [1968] reported the occurrence of a small volcaniclastic basin with associated basaltic dikes in the Central Pyrenees, in the Huesca province in the Iberian domain (Figure 1). Petrological studies by *Galé et al.* [2000] and *Galé and Arranz* [2001] showed the alkaline character of the basaltic lavas. This geochemical affinity may agree with a Cretaceous age, and preliminary ^{87}Rb/^{86}Sr data [*Galé and Arranz*, 2001] suggested an age of ca. 119 Ma.

2.2. Catalonian Coastal Ranges

The Catalonian Coastal Ranges are a NE-SW trending orogen located in the northeastern Iberian plate, next to the coastline (Figure 1). This orogen was constructed by intraplate propagation of the Tertiary Pyrenean compression [*Juez-Larré and Andriessen*, 2002, 2006; *Vergés et al.*, 2002]. The NE area of the orogen is mainly

composed of Paleozoic metasediments and granitoids, whereas the SW zone basically comprises Mesozoic materials; Neogene-Quaternary deposits cover a major proportion of this mountain belt.

In contrast with the Pyrenees, the Cretaceous magmatism in the Catalonian Coastal Ranges is represented only by isolated, alkaline lamprophyres. They intruded into the Paleozoic basement of the northern part of the ranges and cut Late Variscan mafic dykes of subalkaline to transitional affinity and subduction-related signature [*Enrique*, 2009; *Ubide et al*., 2010a, 2011]. The Cretaceous lamprophyres have been found in three zones (Figure 1): a western area [*Pallí et al*., 1993; *Velde and Tournon*, 1970], an eastern area on the coast [*Enrique*, 2009; *Losantos et al*., 2000, 2004; *Ubide et al*., 2012a, 2014], and a central area in between (see section 3.1). Similar to the rocks of the Eastern Pyrenees, these lamprophyres are silica undersaturated [*Enrique*, 2009; *Ubide et al*., 2012a]. They share a common, enriched, and asthenospheric mantle source [*Ubide et al*., 2012b]. The available isotopic ages [*Solé et al*., 2003] correspond to three lamprophyres that vary in age from ca. 80 to 69 Ma. Two of the intrusions were dated by $^{40}K/^{40}Ar$ and one by $^{40}Ar/^{39}Ar$.

3. Samples and Methods

3.1. Location and Description of the Samples

Three outcrops from the Pyrenees and three outcrops from the Catalonian Coastal Ranges were selected for dating with $^{40}Ar/^{39}Ar$ (Figure 1). A total of nine samples were analyzed (Table 1; UTM coordinates in the supporting information tables). The Pyrenean samples comprise one sample from the Basque-Cantabrian Basin (SGR-Bt), one sample from the North Pyrenean Basins (AUB-Amp), and two samples from the Central Pyrenees (DEN1-G and DEN2-G) because it is the least accurately dated domain so far [*Galé and Arranz*, 2001]. No samples were included from the Eastern Pyrenees, as these are the only Cretaceous alkaline rocks in the Pyrenees already dated by the $^{40}Ar/^{39}Ar$ method [*Golberg et al*., 1986; *Vitrac-Michard et al*., 1977] and most of the studies yield very consistent ages [*Golberg et al*., 1986; *Montigny et al*., 1986]. In the Catalonian Ranges, previous data [*Solé et al*., 2003] are scarcer than in the Pyrenees. Accordingly, a total of five samples (CAL-Amp, CAL-G, LLAG-Amp, LLAG-G, and MSPC-Amp) were analyzed from three different, geographically scattered lamprophyre intrusions that have never been dated before.

Sample SGR-Bt is a biotite separate from a gabbro located in the Basque-Cantabrian Basin near Sangroniz (Bilbao). This gabbro intruded the Albian flysch of the Basque Arc domain [*Feuillée and Rat*, 1971]. Petrographically (Figure 2a), it has a medium- to coarse-grained granular holocrystalline texture composed of clinopyroxene, plagioclase, opaque minerals, biotite, apatit,e and secondary phases including calcite, phyllosilicates, and analcime. Sample AUB-Amp is a separate of large amphibole crystals from a monzonite located in the North Pyrenean Basins near L'Aubisqué, south from Pau. This monzonite intruded Albian flysch exposures and can be correlated to the teschenites described previously in this area [e.g., *Azambre et al*., 1992; *Cabanis and Le Fur-Balouet*, 1990]. It shows a coarse-grained holocrystalline doleritic texture (Figure 2b), defined by up to centimeter-sized crystals of feldspars, brown amphibole (kaersutite), which sometimes show green rims, clinopyroxene and opaque minerals with associated biotite; the intergranular spaces are occupied by fine-grained crystals of prehnite, chlorite, analcime and accessory epidote, green amphibole, apatite, acicular feldspars, opaque minerals, and titanite. Samples DEN1-G and DEN2-G are groundmass separates from two basaltic dikes that intrude Devonian metasediments of the Pyrenean Axial Zone in the Central Pyrenees (near Denuy, Huesca) [*Galé et al*., 2000; *Mey*, 1968]. These basalts (Figures 2c and 2d) are highly vesicular fine-grained hypocrystalline porphyritic rocks, where the vesicles are filled with calcite. They carry clinopyroxene, spinel and apatite xenocrysts, and spinel peridotite xenoliths. The groundmass contains plagioclase, biotite, opaque minerals, clinopyroxene, minor amounts of altered glass, and accessory apatite.

The Catalonian Coastal Ranges lamprophyres are subvolcanic intrusions emplaced into Paleozoic rocks in the province of Girona. One of the selected lamprophyres is located near Calella de Palafrugell [see *Ubide et al*., 2010a, 2014 for a full petrological and geochemical characterization of this intrusion]. The second one is located in Llagostera and is reported here for the first time. Although there is only a few meters of exposure, we could study and sample a less weathered underground section during an excavation in the neighboring plot, undertaken for building purposes. The third intrusion is located in the area between Santa Coloma de Farners and Sant Feliu de Buixalleu, near the Monasterio de Sant Pere Cercada [*Pallí et al*., 1993]. The three lamprophyres are classified as camptonites and share similar petrographical features

Table 1. Summary of $^{40}Ar/^{39}Ar$ Data; Preferred Ages are Marked in Bold[a]

Geological Setting	Sample	Separated Phase	Rock Type	Plateau Age (Ma)	±2σ	MSWD	%39Ar, n Steps	Inverse Isochron Age (Ma)	±2σ	MSWD	K/Ca	±2σ
Pyrenees	SGR-Bt	Biotite	Gabbro	104.8	±0.7 ±0.6%	7.64	65.09 8	**101.4**	**±1.2 ±1.2%**	**3.21**	5.602	±1.824
	AUB-Amp	Amphibole macrocrysts	Monzonite	**102.6**	**±0.8 ±0.7%**	**2.06**	99.78 8	102.8	±0.6 ±0.6%	2.29	0.082	±0.005
	DEN1-G	Groundmass	Basalt	**231.8**	**±5.2 ±2.3%**	**2.31**	62.59 5	236.3	±5.7 ±2.4%	2.45	0.067	±0.030
	DEN2-G	Groundmass	Basalt	**179.7**	**±1.4 ±0.8%**	**1.32**	53.23 4	180.7	±1.8 ±1.0%	1.62	0.170	±0.018
Catalonian Coastal Ranges	CAL-G	Groundmass	Lamprophyre	80.7	±1.3 ±1.6%	2.43	74.12 7	79.1	±1.8 ±2.2%	2.40	0.454	±0.048
	CAL-Amp	Amphibole macrocrysts		80.4	±1.4 ±1.7%	37.44	88.70 3	**79.0**	**±0.5 ±0.6%**	**2.34**	0.130	±0.007
	LLAG-G	Groundmass	Lamprophyre	80.4	±0.8 ±1.0%	2.00	64.30 11	**79.2**	**±0.8 ±1.0%**	**1.58**	0.134	±0.017
	LLAG-Amp	Amphibole macrocrysts		78.1	±0.7 ±0.8%	7.26	93.46 3	77.4	±0.9 ±1.1%	7.57	0.128	±0.007
	MSPC-Amp	Amphibole macrocrysts	Lamprophyre	79.5	±0.9 ±1.2%	16.81	99.50 6	**78.2**	**±0.5 ±0.6%**	**1.63**	0.111	±0.004

[a]Full data tables are available in the electronic supplement.

(Figures 2e–2g). They are also very similar to some of the lamprophyres dated by *Solé et al.* [2003]. These rocks are holocrystalline or hypocrystalline, porphyritic due to the presence of millimeter- to centimeter-sized macrocrysts of brown amphibole (kaersutite), clinopyroxene, opaque minerals, and pseudomorphosed olivine. The groundmass is fine grained, especially at the chilled margins of the intrusions where it gets almost aphyric and rich in vesicles. The groundmass is mainly composed of plagioclase, brown amphibole (kaersutite), opaque minerals, acicular apatite, and recrystallized glass (where present). In the lamprophyre from Llagostera, there are evolved patches of groundmass that show K-rich, Ca-poor feldspars and lower volume fractions of mafic minerals. Large amphibole crystals were separated for dating from the three lamprophyres (samples CAL-Amp, LLAG-Amp, and MSPC-Amp). These crystals display homogeneous cores, slightly rounded by magmatic corrosion, and overgrown by subidiomorphic rims (Figures 2e–2g). The groundmass of the lamprophyres from Calella de Palafrugell and Llagostera is especially fine grained (Figures 2e and 2f), and in these cases, groundmass was separated as well for dating experiments (samples CAL-G and LLAG-G).

3.2. $^{40}Ar/^{39}Ar$ Methodology

The selected phases (groundmass, amphibole, or biotite) were separated at the mineral separation laboratory of VU University Amsterdam. Groundmass and amphibole were previously analyzed in order to assure high potassium contents: K_2O varies from 0.54 to 2.27 wt % in groundmass samples—whole rock analyses—and from 1.21 to 2.07 wt % in amphibole crystals—spot analyses. Alteration zones in bulk samples were removed by sawing, and the remaining materials were crushed and sieved to select the 400–500 μm fractions, which were washed with demineralized water. The

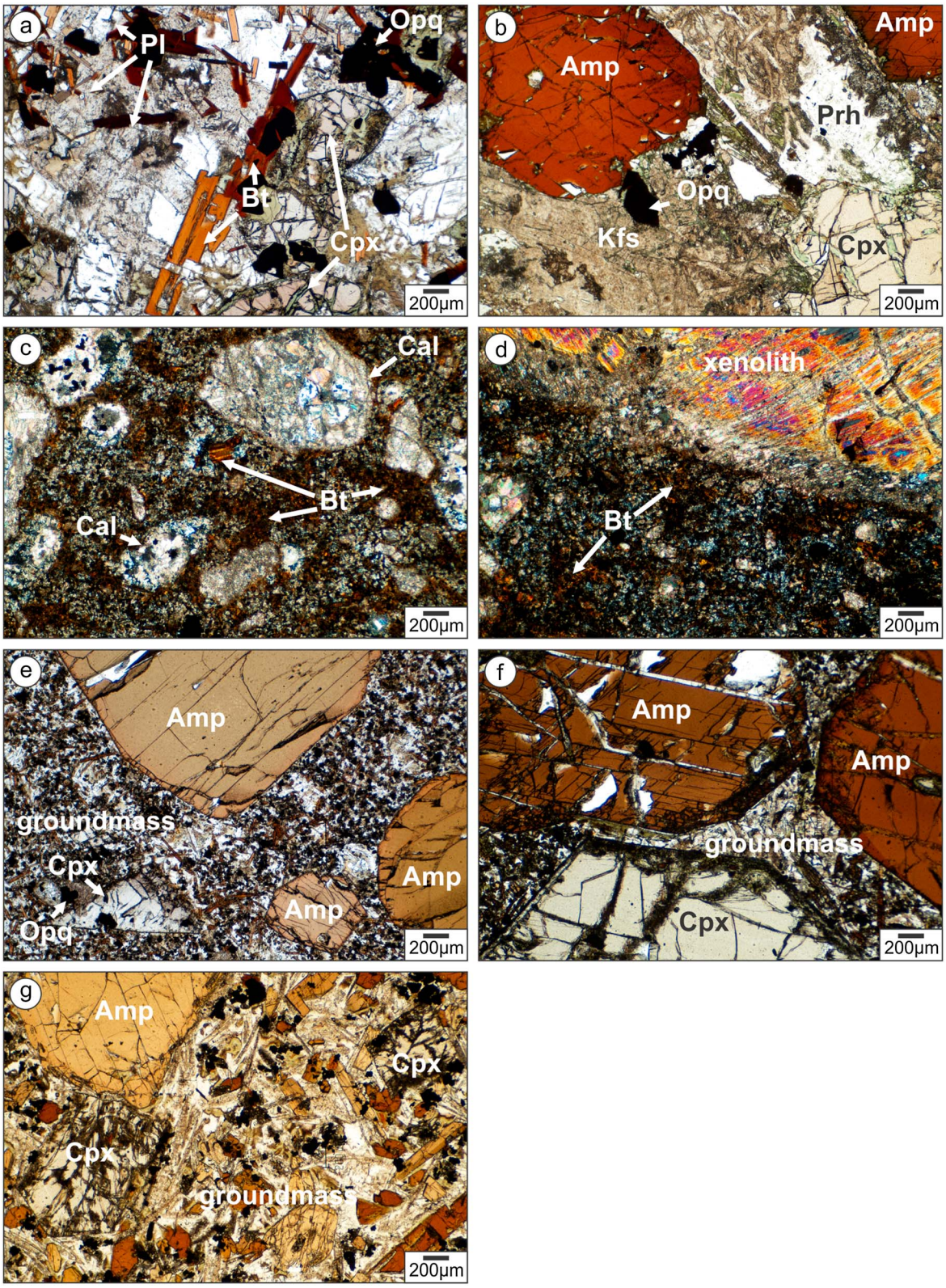

Figure 2. Photomicrographs of the samples dated in this study. Plane-polarized transmitted light (except Figures 2c and 2d, cross-polarized transmitted light). For comparison, the same magnification was used in all the cases. (a) Gabbro from the Basque-Cantabrian Basin (SGR). (b) Monzonite from the North Pyrenean Basins (AUB). (c–d) Basaltic dikes from the Central Pyrenees (DEN1 and DEN2, respectively). (e–g) Lamprophyre intrusions from the Catalonian Coastal Ranges (CAL, LLAG, and MSPC, respectively). Mineral abbreviations are after *Whitney and Evans* [2010].

LOC-50 (Liquid Overflow Centrifuge model-50) [*IJlst*, 1973] was used for heavy liquid separations. Heavy liquids were Diiodomethane diluted with 1.2-Dichlorobenzene. The Frantz® separator was used for magnetic separations. A Faul vibration table was also used when separating biotite. Subsequently, all samples were purified by handpicking under the microscope. Because amphibole and clinopyroxene have very similar appearance and physical properties, an optical method was developed to exclude clinopyroxene grains from amphibole separates [*Ubide et al*., 2010b]. Finally, the samples were cleaned in an ultrasonic bath with demineralized water. Groundmass and amphibole samples were additionally leached with HF (5%, 10 min) to remove alteration from groundmass and overgrowths from amphibole crystals, and cleaned again.

For irradiation, each sample was wrapped in an 8 mm diameter Al foil package. About 30 mg of sample were used for biotite, ca. 50 mg for amphibole and ca. 60 mg for groundmass. Sample packages and 8–10 mg aliquots of laboratory standard sanidine DRA (25.42 Ma, calibrated following *Kuiper et al*. [2008]) wrapped in Cu foil were sealed in a 9 mm diameter ID quartz vial, with one standard package loaded at the top and bottom positions and between every four sample packages. The quartz vial was sealed in a standard Al-irradiation-capsule and irradiated for 20 h in a Cd-lined rotating facility (RODEO) at the NRG-Petten HFR facility in Netherlands.

$^{40}Ar/^{39}Ar$ analyses were carried out at the geochronology laboratory of VU University Amsterdam. The experiments were undertaken on multigrain samples, ca. 9 months after their irradiation, allowing for the decay of ^{37}Ar in Ca-rich samples (groundmass and amphibole). The samples were loaded in 6 mm wide, 3 mm deep holes of 60 mm diameter copper discs, with 21 holes per disc (half of the irradiated material was loaded per sample). The standards were loaded in 3 mm wide, 6 mm deep holes of a 185 holes copper disc (two to three grains per hole and seven replicates per standard). The samples and the standards were preheated to ca. 200°C to remove undesirable atmospheric argon. After this preheating step, they were placed in an ultrahigh vacuum extraction line. A CO_2 laser heating system was used for all the experiments; single fusion was applied to the standards and incremental heating to the samples. Positioning of the laser beam was achieved using an analogue Raylease scanhead fitted with a dual mirror system for *X*–*Y* adjustment and a ZnS 300 mm focusing lens. The beam delivery system achieved ca. 300 μm at the focal point and for the samples the beam was diffused in the *y* direction with a 200 Hz frequency triangular current causing a +1 and −1 mm beam deflection. To ensure even heating of all the grains, the beam was applied in circles increasing in diameter for the standards and in a raster pattern for the samples. The gas was analyzed isotopically with a Mass Analyzer Products LTD 215-50 noble gas mass spectrometer. Beam intensities of Ar isotopes were measured in a magnet field controlled peak-jumping mode over the mass range 40–36 on a secondary electron multiplier using switchable amplifier resistors with relative gains of 5×10^2, 5×10, and 5 with respect to the Faraday collector (10^{11} Ω resistor on the Faraday collector amplifier). For data collection, the mass spectrometer is operated with a modified version of standard MAP software. System blanks were measured every two (biotite) or four (groundmass and amphibole) sample measurements and at the beginning and the end of each step. The total system blanks were in the range of 6×10^{-2}–9×10^{-1} volts for mass 40, 5×10^{-5}–6×10^{-3} volts for mass 39, 8×10^{-6}–7×10^{-4} volts for mass 38, 1×10^{-5}–2×10^{-4} volts for mass 37, and 2×10^{-4}–4×10^{-3} volts for mass 36. Mass discrimination (ca. 1.002–1.010 per atomic mass unit and 1.0045 for the main series of experiments) was monitored by frequent analysis of $^{40}Ar/^{36}Ar$ air pipette aliquots.

Data reduction was performed with the originally in-house-developed ArArCalc2.5 software package [*Koppers*, 2002] (http://earthref.org/tools/ararcalc/). Each analysis was corrected for mass discrimination; system blanks were negligible compared to sample signals (often better than a factor of per mil). The irradiation parameter J for each sample was determined by interpolation using a second-order polynomial fitting between the individually measured standards. For the decay constants and the abundance of ^{40}K, the values recommended by the IUGS Subcommission on Geochronology [*Steiger and Jäger*, 1977] were used.

4. Results

A summary of $^{40}Ar/^{39}Ar$ incremental heating results is presented in Table 1. Full data tables can be found in the supporting information tables, where the results are reported following recommendations by *Renne et al*. [2009]. Age spectra, K/Ca spectra, and inverse isochron plots are presented in Figure 3, with uncertainties quoted at 2σ.

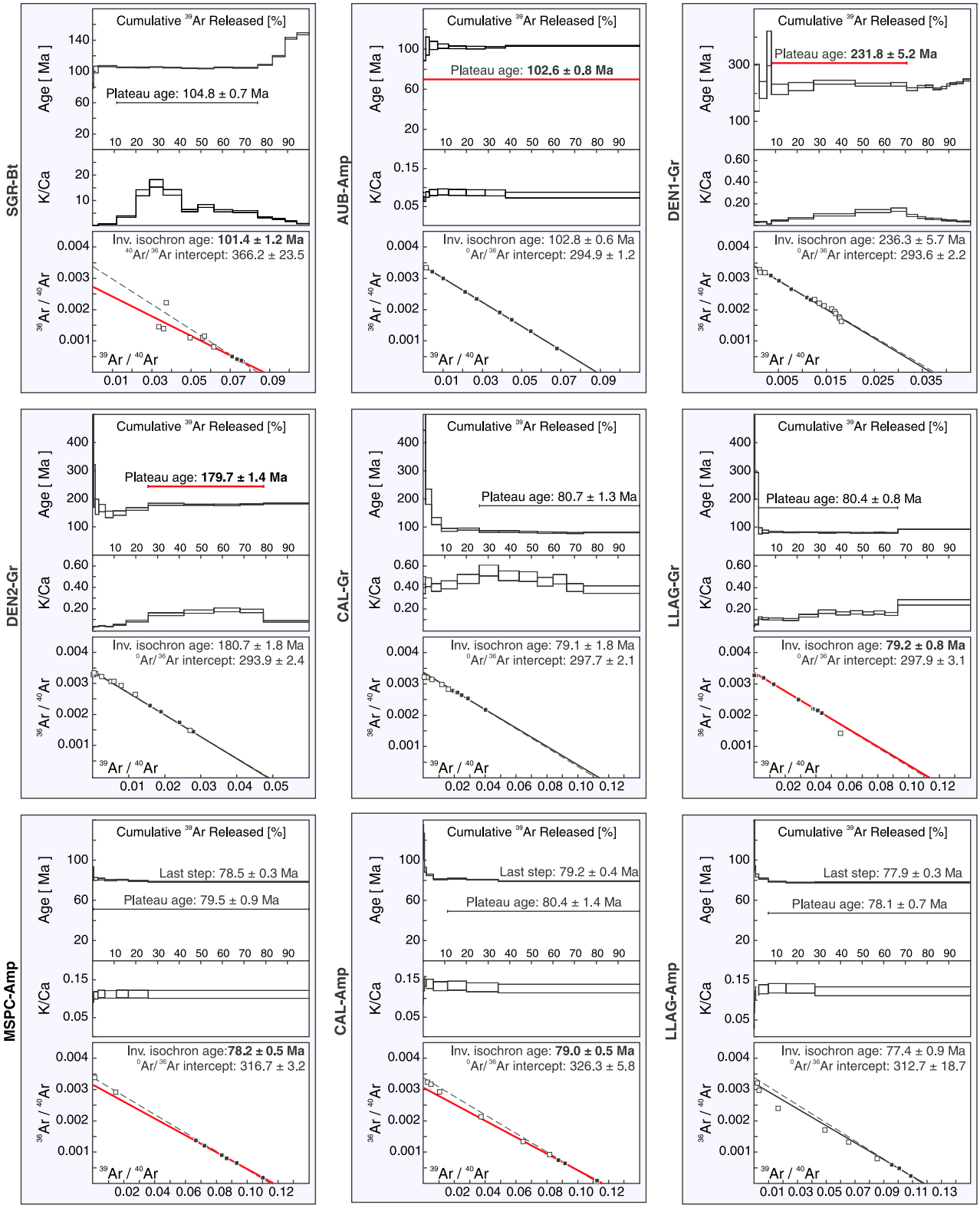

Figure 3. $^{40}Ar/^{39}Ar$ incremental heating results, presented in age and K/Ca spectra and inverse isochron plots. In the age and K/Ca spectra, the thickness of the steps reflects the associated uncertainty; the horizontal line represents the plateau. In the inverse isochron diagrams, the dashed line represents the ideal atmospheric-radiogenic mixing line, whereas the solid line represents the inverse isochron calculated with the plateau defining steps (black squares); square size includes uncertainty. The preferred crystallization age is marked in bold and graphically with a thicker red line. The age obtained from the last step is included for samples MSPC-Amp, CAL-Amp, and LLAG-Amp (amphibole separate samples from the Catalonian Coastal Ranges).

Our experiments showed good, consistent results with age calculations that in most cases meet commonly accepted reliability criteria [*McDougall and Harrison*, 1999]. Several age spectra showed elevated ages in the initial steps which may either point to loosely bound excess ^{40}Ar (some amphibole separates) or, alternatively, to recoil loss of ^{39}Ar from fine-grained alteration phases (some groundmass separates) [*Koppers et al*., 2000; *Wijbrans et al*., 2007]. The first steps were not considered in the age calculations if they contained abundant atmospheric argon, excess argon, were affected by recoil loss of ^{39}Ar, or presented large uncertainties. The last steps were not considered in the age calculations if they revealed extraneous (excess or inherited) argon. Always three or more concordant, contiguous, high-temperature steps were selected, representing more than 50% of the ^{39}Ar released.

If the ^{40}Ar/^{36}Ar intercept for the trapped argon derived from the isochron treatment of the data was not significantly different from the atmospheric ratio of 295.5, excess argon was ruled out (groundmass separates and sample AUB-Amp) and the preferred age was chosen according to the mean squares of weighted deviates (MSWD) values, which measure the extent to which the scatter of data can be explained by analytical uncertainty. In contrast, if excess argon was detected (biotite and some amphibole separates), the inverse isochron age was preferred over the plateau age [e.g., *McDougall and Harrison*, 1999].

Preferred crystallization ages (plateau or inverse isochron ages) are marked in bold in Table 1 and Figure 3. All preferred ages show MSWD values below the cutoff value of 2.5 [*O'Connor et al*., 2007] excepting sample SGR-Bt, which nevertheless presents an acceptable inverse isochron age.

From the amounts of ^{39}Ar and ^{37}Ar released during the experiments, some information may be obtained on the chemical composition of the mineral phases contributing to the spectrum [*Wijbrans et al*., 2007]. This effect is shown in the K/Ca plots (Figure 3). The variation in K/Ca is never larger than 1 order of magnitude, highlighting the purity of the separates. Meanwhile, the radiogenic component of the argon in the selected steps ranges from less than 10% to almost 100%. It is generally very high for biotite and amphibole separates and rather low for groundmass separates, although this is not reflected in larger analytical uncertainties in the groundmass experiments.

The detailed interpretation of the age results is in the supporting information appendix. Sample SGR-Bt from the Basque-Cantabrian Basin and AUB-Amp from the North Pyrenean Basins yielded similar Albian ages at 101.4 ± 1.2 and 102.6 ± 0.8 Ma, respectively (Figure 3 and Table 1). In the Central Pyrenees, samples DEN1-G and DEN2-G yielded different ages, neither of them Cretaceous (Figure 3 and Table 1). The age of DEN1-G is 231.8 ± 5.2 Ma (Late Triassic) and that of DEN2-G is 179.7 ± 1.4 Ma (Early Jurassic). Finally, in the Catalonian Coastal Ranges, all the experiments yielded similar Campanian ages at ca. 79 Ma (Figure 3 and Table 1). Groundmass and amphibole separates yielded ages indistinguishable from each other within the uncertainty. The preferred crystallization age for each intrusion was 79.0 ± 0.5 Ma for the lamprophyre from Calella de Palafrugell (CAL-Amp sample), 79.2 ± 0.8 Ma for the lamprophyre from Llagostera (LLAG-G sample), and 78.2 ± 0.5 Ma for the lamprophyre from the Monasterio de Sant Pere Cercada (MSPC-Amp sample).

5. Discussion

5.1. The Triassic-Jurassic Rifting in the Central Pyrenees

The age of the basaltic dykes of the Central Pyrenees (samples DEN1-G and DEN2-G) is Late Triassic (ca. 232 Ma; Carnian) and Early Jurassic (ca. 180 Ma; Toarcian), respectively (Table 1). These dykes were sampled given their alkaline composition to test if their preliminary Cretaceous age (^{87}Rb/^{86}Sr dating) [*Galé and Arranz*, 2001] was correct, but our ^{40}Ar/^{39}Ar results dismiss that hypothesis.

During the Triassic and Jurassic, two types of magmatic events are recognized in northeast Iberia. On the one hand, there is widespread tholeiitic magmatism (ophites) emplaced during the Triassic-Jurassic boundary in the Western and Central Pyrenees [e.g., *Alibert*, 1985; *Azambre et al*., 1987; *Béziat et al*., 1991; *Montigny et al*., 1982; *Rossi et al*., 2003]. On the other hand, there is a Late Triassic alkaline igneous province [*Lago et al*., 1996; *Sanz et al*., 2013, and references therein] comprising magmatic occurrences scattered in the Iberian Chain, the Catalonian Coastal Ranges, and the Eastern Pyrenees with a Norian age [*Montigny et al*., 1982].

Our geochronological results reveal for the first time a Triassic-Jurassic phase of alkaline magmatism in the Central Pyrenees. Given the affinity of these rocks, one could think they have a common origin within the

alkaline igneous province. The differences in age between our samples (ca. 50 Ma) suggest this phase of magmatism was likely multiepisodic. If related to the alkaline province, the whole province would cover a longer time span than previously thought. This kind of enduring, sporadic, scattered, low volume, and geochemically homogeneous magmatism has recently been documented in the nearby Languedoc volcanic province [*Dautria et al*., 2010], where alkali basaltic activity spans from 161 to 0.5 Ma. More data would be necessary to constrain the Triassic-Jurassic alkaline activity in the Pyrenees.

Azambre and Fabriès [1989] proposed that the tholeiitic and alkaline Triassic magmatic events developed in a context of continental rifting which affected southwestern Europe after the Variscan orogeny, at the beginning of the Alpine cycle. According to these authors, the tholeiitic magmatism represents the greatest effects of rifting and intruded subsiding Triassic basins. More recently, the tholeiitic magmatism has been related to the Central Atlantic Magmatic Province (CAMP) [*Rossi et al*., 2003]. In contrast, the alkaline magmatism developed at the same time along the boundaries of the subsiding Triassic basins with adjacent blocks and represents off-axis magmatism [*Azambre and Fabriès*, 1989]. The subsiding basins developed from ca. 240–220 Ma to the Mesozoic and part of the Cenozoic in the Eastern Pyrenees [*Azambre and Fabriès*, 1989], and there is also Late Triassic–Early Jurassic subsidence documented in the Catalonian Coastal Ranges [*Juez-Larré and Andriessen*, 2002, 2006; *Solé et al*., 1998]. Strikingly, the initiation age of the basins coincides with our oldest result at ca. 232 Ma (Table 1). Therefore, this alkaline magmatism started coevally with the subsidence at the Late Triassic and was also active in the Early Jurassic (ca. 180 Ma, Table 1).

5.2. The Cretaceous Opening of the Bay of Biscay and Rotation of Iberia

The results obtained for the Cretaceous alkaline magmatism in northeast Iberia are clearly arranged in two, very consistent groups (Table 1): the ages obtained in the Pyrenees point to ca. 102 Ma (Late Albian), whereas those from the Catalonian Coastal Ranges agree at ca. 79 Ma (Campanian). We have plotted our Cretaceous ages together with the results of previous geochronological studies in the chronostratigraphic chart of Figure 4. Our data show significantly smaller uncertainties and are within the wide range defined by previous data, most of which correspond to $^{40}K/^{40}Ar$ analyses.

This section will be focused on the Pyrenean ages. The most relevant previous study was carried out by *Montigny et al*. [1986] with rocks from the whole Pyrenean chain. According to these authors, magmatic activity took place between 110 and 85 Ma (Figure 4), with most data within the interval between 100 and 90 Ma and younger data (ca. 90–85 Ma) restricted to samples from the western part of the belt. These authors report six ages around 110 Ma in the central part of the North Pyrenean Zone that are problematic because they are older than their country rock (Albian-Cenomanian flysch) [*Dubois and Seguin*, 1978] and also older than genetically related extrusive rocks [*Dubois and Seguin*, 1978; *Schoeffler et al*., 1964] (see Figure 4). Furthermore, they recognize excess Ar in other minerals analyzed from the same rocks. We will therefore not consider these ages further in the discussion. In the Eastern Pyrenees, consistent data by *Golberg et al*. [1986] and *Montigny et al*. [1986] constrain the age of the magmatism to ca. 95–90 Ma (Figure 4), updating a younger age obtained by *Vitrac-Michard et al*. [1977] that will not be considered further in the discussion. Regarding the age of the extrusive rocks, they crop out in the Basque-Cantabrian Basin and North Pyrenean Basins and their stratigraphic position agrees with the main magmatic phase at 100–90 Ma and also with the more recent ages in the Basque-Cantabrian Basin [*Castañares and Robles*, 2004; *Dubois and Seguin*, 1978; *Schoeffler et al*., 1964] (Figure 4). Additionally, an Early Albian extrusive phase is recognized in the Basque-Cantabrian Basin [*Fernández-Mendiola and García-Mondéjar*, 2003].

The evaluation of previous data reveals that the Cretaceous magmatism in the Pyrenees is Albian to Santonian, mostly 105–85 Ma (instead of 110–85 Ma considering the work by *Montigny et al*. [1986] or 110–82 Ma considering the whole data set; Figure 4). The 105–85 Ma range includes most acceptable isotopic and stratigraphic ages and covers the Basque-Cantabrian Basin, the North Pyrenean Basins, and the Eastern Pyrenees. New geochronological data obtained in the present study have uncertainties significantly lower than previous results and agree at ca. 102 Ma (Figure 4). According to the integration of new and revisited data, the magmatism must not be considered Albian to Turonian as frequently cited [e.g., *Gong et al*., 2009; *Vissers and Meijer*, 2012a] although the magmatic activity concentrated especially in the range ca. 100–90 Ma. Another interesting feature is that the magmatism is very limited in time in the Eastern Pyrenees (95–90 Ma), whereas multiple stages are recognized toward the west with the longest time span recorded in the Basque-Cantabrian Basin (Figure 4); this is in good agreement with the propagation of the V-shaped Bay of Biscay rift.

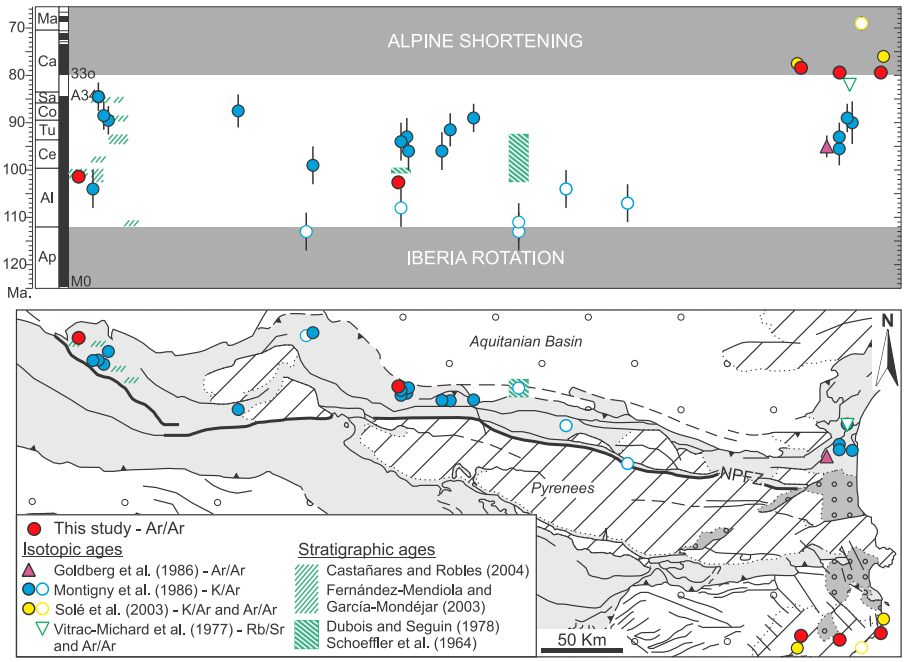

Figure 4. Summary of ages for the Cretaceous magmatism in northeast Iberia. The horizontal position of each age correlates with its location in the geological map below (simplified from Figure 1). Red circles represent the samples dated in this study. The other symbols represent data from the literature (white-filled symbols are discarded data; see sections 5.2 and 5.3). Isotopic ages correspond to intrusive rocks, whereas stratigraphic ages correspond to extrusive rocks. Vertical lines represent the uncertainty associated to isotopic ages (for our data, symbol size includes uncertainty). The rotation of Iberia took place during the Aptian [*Gong et al.*, 2008] and the mainly Tertiary Alpine compression started in the Late Cretaceous [e.g., *Vissers and Meijer*, 2012b]. The geological timescale and the geomagnetic polarity timescale are from *Walker and Geissman* [2009]. Note the Cretaceous Normal Superchron between magnetic anomalies M0 and A34. Ap: Aptian; Al: Albian; Ce: Cenomanian; Tu: Turonian; Co: Coniacian; Sa: Santonian; Ca: Campanian; Ma: Maastrichtian.

Contemporaneous with the magmatic activity, mantle exhumation, LP/HT metamorphism, and hydrothermal activity are recognized in the North Pyrenean Zone, close to the North Pyrenean Fault Zone [*Golberg et al.*, 1986; *Lagabrielle and Bodinier*, 2008; *Lagabrielle et al.*, 2010; *Montigny et al.*, 1986; *Poujol et al.*, 2010; *Schärer et al.*, 1999]. In particular, the subcontinental mantle crops out as restricted bodies of ultramafic rocks, crosscut in certain areas by a late generation of amphibole-pyroxenite veins [*Lagabrielle and Bodinier*, 2008, and references therein]. These veins are considered to represent melt conduits for the Cretaceous alkaline magmatism in the Pyrenees [*Golberg et al.*, 1986; *Bodinier et al.*, 1987]. $^{40}Ar/^{39}Ar$ dating of amphibole from the veins provided ages of ca. 103 Ma [*Albarède and Michard-Vitrac*, 1978], ca. 101 Ma [*Golberg et al.*, 1986], and ca. 108–103 Ma [*Henry et al.*, 1998], and unpublished results of the VU argon laboratory are also similar. These data are in line with the main magmatic phase at ca. 100–90 Ma and especially with our new ages at ca. 102 Ma, supporting the link between the amphibole veins and the Cretaceous magmas.

The Cretaceous magmatism, metamorphism, hydrothermalism, and mantle exhumation are related to a context of crustal extension and extreme thinning along the North Pyrenean Zone, linked to the opening of the Bay of Biscay and allied rotation of Iberia with respect to Europe [e.g., *Jammes et al.*, 2009; *Lagabrielle and Bodinier*, 2008; *Lagabrielle et al.*, 2010; *Montigny et al.*, 1986; *Poujol et al.*, 2010]. However, considering that the rotation of Iberia has recently been confined to the Aptian [*Gong et al.*, 2008] (see Figure 4), all these events are not simultaneous with the rotation as traditionally considered [e.g., *Cabanis and Le Fur-Balouet*, 1990; *Montigny et al.*, 1986], but postrotation. They therefore developed in a tectonically unclear stage in the Iberia motion, after the Aptian rotation and before the onset of the Alpine compression in the Late Cretaceous. The ages of magmatic rocks in the Pyrenees define a time-band between both tectonic events (Figure 4).

Regarding the kinematics of opening of the Bay of Biscay and consequent rotation of Iberia, two end-member models have been put forward. Both models achieve a good fit between the shape of the northern

and southern Bay of Biscay continental margins. The differences are mainly in deriving the Euler poles of the rotation, which are required for the kinematic reconstructions.

The first model is based on the fit of sea-floor magnetic anomalies across the North Atlantic and Bay of Biscay and is supported by paleomagnetic data and plate-kinematic analysis [*Sibuet et al*., 2004; *Srivastava et al*., 2000; *Vissers and Meijer*, 2012a]. It proposes a scissor-type opening for the Bay of Biscay which leads to ca. 35° of counterclockwise rotation of Iberia. The main drawback of this model is that it implies large-scale convergence in the Pyrenean domain, which in principle is not consistent with the subsequent development of flysch-filled basins, magmatism, metamorphism, hydrothermalism, and mantle exhumation in the North Pyrenean Zone. *Vissers and Meijer* [2012a] solve some of these objections by proposing a scissor-type opening model in which the convergence in the Pyrenean realm was accommodated by up to 300 km of north-directed subduction underneath the European margin. According to this work, the lithosphere subducted during the Aptian rotation became gravitationally unstable during the subsequent stagnant stage and detached in the Albian, leading to asthenospheric upwelling and consequent magmatism, metamorphism, and extension in the overlying European margin now exposed in the North Pyrenean Zone [*Vissers and Meijer*, 2012a]. These authors relate the lack of evidence for subduction in the Pyrenees to the fact that the subducted crust was amagmatic, mantle-dominated ocean floor exhumed under conditions of ultraslow spreading during the Late Jurassic and Early Cretaceous. In this model, sedimentary basins and magmatism are triggered by asthenospheric upwelling, implying an "active rifting" scenario [e.g., *Wilson*, 1989].

A second end-member model is based on geological evidence for extension in Pyrenean basins and proposes a dominantly left-lateral strike-slip motion between Iberia and Europe, with Iberia moving in a southeasterly direction along the North Pyrenean Fault Zone [*Choukroune*, 1992; *Oliva-Urcia et al*., 2011; *Olivet*, 1996]. This model, however, is not consistent with sea-floor reconstructions and implies significantly less than the ca. 35° counterclockwise rotation documented by paleomagnetism [*Gong et al*., 2008]. In this model, the transtensional setting leads to crustal thinning that triggers the magmatism in a "passive rifting" scenario [e.g., *Wilson*, 1989].

A third, alternative kinematic model has been recently proposed by *Jammes et al*. [2009, 2010] based on field data in the western Pyrenees together with previous observations and numerical modeling. This model proposes a scissor-type opening for the Bay of Biscay with an inferred pole of rotation located in the Mediterranean Sea, preceded by a left-lateral strike-slip motion between Iberia and Europe during the Late Jurassic to Early Cretaceous. The main advantage of this model is that the rotation pole in the Mediterranean sea produces scissor-type opening in the Bay of Biscay as well as in the Pyrenean domain, explaining extension in the North Pyrenean Zone and the formation of the Cretaceous basins. However, as in the strike-slip opening case, the model is not consistent with sea-floor reconstructions and implies significantly less than the ca. 35° counterclockwise rotation documented by paleomagnetism [*Gong et al*., 2008; see *Vissers and Meijer*, 2012a]. In this case, the purely extensional setting in the North Pyrenean Zone favored crustal thinning and magmatism in a "passive rifting" scenario [e.g., *Wilson*, 1989].

Given that the Cretaceous alkaline magmatism follows the rotation and separation of Iberia from Europe (Figure 4), the temporal, geographical and petrological distribution of the igneous rocks may shed some light on the long-standing debate regarding the kinematics of opening of the Bay of Biscay. The chronological distribution of the magmatism reveals slight differences along the Pyrenees, with more magmatic stages and a more enduring magmatic activity toward the west (Figure 4). Furthermore, the magmatism is widespread and mainly extrusive in the west (Basque-Cantabrian Basin) but becomes progressively scarcer and more intrusive toward the east, with no extrusive rocks cropping out in the Eastern Pyrenees; this could also be related to a deeper erosion level for the eastern sector. Finally, the nature of the magmatism is different, with silica undersaturated rocks to the east, related to a lower melting rate of the mantle source [e.g., *Cabanis and Le Fur-Balouet*, 1990]. These lines of evidence suggest that extension was more developed and long-lasting toward the west. Such a tectonic variability along the Pyrenees appears to support a scissor-type opening model for the Bay of Biscay.

The magmatism studied is associated to a continental rift setting. Hence, the mechanism of initiation of rifting can also be evaluated to test the kinematics of opening for the Bay of Biscay. Although "active rifting" versus "passive rifting" are extreme mechanisms and too simplistic to be applied straightforwardly to the

interpretation of rift systems, several lines of evidence point to a "passive rifting" scenario, namely, (i) the magmatism is simultaneous or postdates the Albian-Cenomanian flysch sequences filling the North Pyrenean Basins (Figure 4), (ii) the volume of magmatism is relatively small and major focus of volcanism is restricted to the Basque-Cantabrian Basin, and (iii) there are no subalkaline or transitional flood basalts that would point to a thermal anomaly within the upper mantle. Furthermore, in the review on rift evolution by *Ziegler and Cloetingh* [2004], mantle upwelling is considered a consequence of lithospheric extension and not the main driving force of rifting.

To sum up, the varying geochronological, petrological, and compositional characteristics of the magmatisms along the belt support a scissor-type opening model and the relative timing of extension and magmatism reveal a "passive rifting" scenario, supporting the model by *Jammes et al*. [2009, 2010]. Plate-kinematic results, however, disagree with this reconstruction [*Vissers and Meijer*, 2012a]. It is clear that more data are necessary to develop a consensus model for the kinematic evolution of Iberia, as suggested recently by *Neres et al*. [2013].

5.3. The Onset of the Alpine Compression in the Late Cretaceous

Samples from the Catalonian Coastal Ranges yield the youngest ages, constraining the magmatic activity in this setting to the Campanian, at ca. 79 Ma (Figure 4 and Table 1). This datum is very well defined as macrocryst and groundmass separates yield consistent ages in all the studied intrusions (see section 4). The previous geochronological study by *Solé et al*. [2003] provided three ages, including an especially young one (ca. 69 Ma) which is not supported by our data and as noted by those authors, must be considered a minimum estimate.

The Cretaceous magmatism in the Catalonian Coastal Ranges is the only located in the Iberian domain, to the south of the North Pyrenean Fault Zone, and is significantly younger than the ca. 95–90 Ma age of the igneous rocks from the Eastern Pyrenees (Figure 4). Strikingly, its age at ca. 79 Ma coincides with the age of magnetic anomaly 33o [e.g., *Gee and Kent*, 2007; *Walker and Geissman*, 2009] (Figure 4). *Solé et al*. [2003] stated that these magmas were emplaced in zones of crustal relaxation and/or thinning in the relatively stable tectonic transition between the rotation of the Iberian Peninsula and the Alpine collision with respect to Europe. It is however unclear when exactly Alpine compression commenced.

The change to a transpressional regime is well recorded in the Pyrenean geology by inversion of previous extensional faults and deposition of growth sequences in the south-central Pyrenees [*Beaumont et al*., 2000; *Choukroune*, 1992; *García-Senz*, 2002; *Garrido-Megías and Ríos-Aragüés*, 1972; *López*, 2013; *McClay et al*., 2004; *Muñoz*, 1992; *Puigdefàbregas and Souquet*, 1986]. However, these authors report slightly different ages from the Santonian to the Maastrichtian for the onset of compression. Recent studies to the north of the Pyrenees suggest that the first synorogenic deposits are Early Campanian [e.g., *Lavenu et al*., 2013; *Leleu et al*., 2009]. According to plate-kinematic reconstructions based on the fit of sea-floor magnetic anomalies, *Rosenbaum et al*. [2002] concluded that the relative motion of Iberia and Europe changed to convergence at anomaly A34 (85 Ma, Santonian, according to the timescale by *Walker and Geissman* [2009]; Figure 4). The recent kinematic studies by *Vissers and Meijer* [2012a, 2012b] emphasized that there is no geological evidence in the Pyrenees for any significant crustal shortening prior to the Campanian. *Vissers and Meijer* [2012b] proposed that the onset of collision was coeval with the latest stages of spreading in the Bay of Biscay, which involved first extension then shortening in the Pyrenean domain with a sinistral strike-slip component. Specifically, strike-slip shortening started at anomaly 33o.

Our geochronological results consistently point to a magmatic event at 79 Ma (Figure 4). This is inconsistent with Alpine shortening starting before that time. Indeed, the timing of the magmatism coincides exactly with the abovementioned change of tectonic regime in the Pyrenean domain, from strike-slip extension to strike-slip shortening, at anomaly 33o [*Vissers and Meijer*, 2012b]. Moreover, detrital thermochronometry of foreland basin sediments gives insights on the early stage of orogenic development [e.g., *Filleaudeau et al*., 2012], and recent studies in the south-central Pyrenees identify a first exhumation signal at ca. 78 Ma [*Whitchurch et al*., 2011] and ca. 80 Ma [*Filleaudeau et al*., 2012], well in line with the age of the magmatism as well.

Lamprophyre intrusions are commonly associated to strike-slip shear zones [*Pirajno*, 2010, and references therein]. *Scarrow et al*. [2006, 2011] proposed that lamprophyres potentially act as tectonomagmatic markers

of changes in geodynamic conditions. These authors studied Permian alkaline lamprophyres in the Central Iberian Zone, emplaced in a transpressional to transtensional tectonic regime during the transition between the Variscan and the Alpine cycles. *Gil-Imaz et al*. [2012] showed the relationship between Permian lamprophyre emplacement and change in stress regime from transpression to transtension in the Pyrenees. Also, the emplacement of the Cretaceous alkaline lamprophyres from the Western Iberian Margin has been recently linked to the onset of Alpine convergence between the African and Iberian plates [*Miranda et al*., 2009].

In the Catalonian Coastal Ranges, lamprophyre intrusions at ca. 79 Ma (Campanian, anomaly 33o) appear to correlate with the change between strike-slip extension and strike-slip shortening. Since Alpine compression started at the Iberia-Europe plate boundary and was propagated into the plate interiors afterward, the age of the magmatism in the Catalonian Coastal Ranges could be subsequent to the onset of compression at the plate margin. However, tectonic inversion in the Catalonian Coastal Ranges is considered Late Cretaceous as well [*Juez-Larré and Andriessen*, 2002, 2006] and the magmatism is located in the Paleozoic basement at the northernmost tip of the Ranges (see Figure 1), so probably within the Pyrenean realm during Late Cretaceous times. Moreover, the Pyrenean orogen developed diachronously from east to west [*Whitchurch et al*., 2011, and references therein] and values for the total shortening across the belt tend to increase toward the east [e.g., *Vergés et al*., 2002], consistently with a small component of counterclockwise rotation of Iberia during convergence [*Vissers and Meijer*, 2012b]. These data lend further support to considering the lamprophyres from the Catalonian Coastal Ranges as indicators of tectonic change to Alpine strike-slip shortening in northeasternmost Iberia.

6. Conclusions

New $^{40}Ar/^{39}Ar$ ages on the magmatism of the Pyrenees and Catalonian Coastal Ranges form three age groups: a Late Triassic (ca. 232 Ma)–Early Jurassic (ca. 180 Ma) magmatism in the Central Pyrenees that was previously thought to be Cretaceous, a Cretaceous (ca. 102 Ma) magmatism in the Basque-Cantabrian Basin and the North Pyrenean Basins, and a Late Cretaceous (ca. 79 Ma) magmatism in the northern part of the Catalonian Coastal Ranges. These results, combined with a detailed evaluation of previous data, provide new insights into the geodynamic evolution of northeast Iberia during the Alpine cycle:

1. The Late Triassic and Early Jurassic ages represent the first report of an alkaline magmatism in the Central Pyrenees for that time. The new ages widen temporally and geographically the alkaline magmatism associated to the continental rift setting developed in northeast Iberia and in general southwest Europe after the end of the Variscan orogeny.
2. The Cretaceous alkaline magmatism in the Pyrenees took place from the Albian to the Santonian (mostly between 105 and 85 Ma). In contrast with traditional thinking, magmatism is not coeval but postdates the Aptian rotation of Iberia with respect to Europe, which is related to the opening of the Bay of Biscay. Magmatism as well as contemporaneous metamorphism, hydrothermalism, and mantle exhumation developed in a tectonically unclear stage between the rotation of Iberia and the onset of Alpine collision. Magmatic activity is especially recorded between ca. 100 and 90 Ma. It is restricted to ca. 95–90 Ma in the Eastern Pyrenees, whereas multiple stages develop toward the west with the longest time span recorded in the Basque-Cantabrian Basin. Our new ages at ca. 102 Ma agree with those of amphibole in veins that crosscut mantle exposures, supporting the interpretation that the veins represent melt conduits for the Cretaceous alkaline magmas.
3. The Late Cretaceous alkaline magmatic event in the Catalonian Coastal Ranges is precisely dated at ca. 79 Ma (Campanian). This age is inconsistent with shortening starting before that time as previously considered and thus may represent the onset of the Alpine shortening in northeast Iberia.

Acknowledgments

We are grateful to Suzon Jammes, Jesús Solé, and two anonymous reviewers as well as Editors John Geissman, Onno Oncken, and Paola Vannucchi for useful comments and suggestions that helped improve the original manuscript. We warmly thank Roel van Elsas (VU Amsterdam) for assistance during mineral separation and Carles Roqué and Lluis Pallí (Universitat de Girona) for advice on sampling localities in the Catalonian Coastal Ranges. We are indebted to Anna Ferrer, who kindly provided access to the underground section of the lamprophyre in Llagostera. This work was supported by the research project CGL2008-06098/BTE (MICINN, Spain) and is included in the scope of the predoctoral grant BFI06.189 (Gobierno Vasco) to Teresa Ubide; this institution provided additional funding for research stays at VU University Amsterdam to carry out mineral separation and $^{40}Ar/^{39}Ar$ dating. We acknowledge the Gobierno de Aragón, supporting the research group Geotransfer.

References

Albarède, F., and A. Michard-Vitrac (1978), Age and significance of the North Pyrenean metamorphism, *Earth Planet. Sci. Lett.*, *40*, 327–332, doi:10.1016/0012-821X(78)90157-7.

Alibert, C. (1985), A Sr-Nd isotope and REE study of Late Triassic dolerites from the Pyrenees (France) and the Messejana Dyke (Spain and Portugal), *Earth Planet. Sci. Lett.*, *73*, 81–90, doi:10.1016/0012-821X(85)90036-6.

Azambre, B., and J. Fabriès (1989), Mesozoic evolution of the upper mantle beneath the eastern Pyrenees: Evidence from xenoliths in Triassic and Cretaceous alkaline volcanics of the eastern Corbières (France), *Tectonophysics*, *170*(3–4), 213–230, doi:10.1016/0040-1951(89)90272-2.

Azambre, B., M. Rossy, and M. Lago (1987), Petrology of tholeiitic Triassic dolerites (ophites) from the Pyrenees, *Bull. Mineral.*, *110*(4), 379–396.

Azambre, B., M. Rossy, and F. Albarède (1992), Petrology of the alkaline magmatism from the Cretaceous North-Pyrenean Rift Zone (France and Spain), *Eur. J. Mineral.*, *4*, 813–834.
Beaumont, C., J. A. Muñoz, J. Hamilton, and P. Fullsack (2000), Factors controlling the Alpine evolution of the central Pyrenees inferred from a comparison of observations and geodynamical models, *J. Geophys. Res.*, *105*(B4), 8121–8145, doi:10.1029/1999JB900390.
Béziat, D., J. L. Joron, P. Monchoux, M. Treuil, and F. Walgenwitz (1991), Geodynamic implications of geochemical data for the Pyrenean ophites (Spain-France), *Chem. Geol.*, *89*(3–4), 243–262, doi:10.1016/0009-2541(91)90019-N.
Bodinier, J. L., J. Fabriès, J. P. Lorand, J. Dostal, and C. Dupuy (1987), Geochemistry of amphibole pyroxenite veins from the Lherz and Freychinède ultramafic bodies (Ariège, French Pyrénées), *Bull. Mineral.*, *110*, 345–358.
Bullard, E. C., J. E. Everett, and A. G. Smith (1965), The fit of the continents around the Atlantic, *Philos. Trans. Roy. Soc. A*, *258*, 41–51, doi:10.1098/rsta.1965.0020.
Cabanis, B., and S. Le Fur-Balouet (1990), Le magmatisme crétacé des Pyrénées – Apport de la géochimie des éléments en traces – Conséquences chronologiques et géodynamiques, *Bull. Centres Rech. Explor.-Prod. Elf-Aquitaine*, *14*(1), 155–184.
Carey, W. S. (1958), The orocline concept in Geotectonics, *Proc. R. Soc. Tasmania*, *89*, 255–288.
Carracedo-Sánchez, M., F. Sarrionandia, T. Juteau, and J. I. Gil-Ibarguchi (2012), Structure and organization of submarine basaltic flows: Sheet flow transformation into pillow lavas in shallow submarine environments, *Int. J. Earth Sci. (Geol. Rundsch.)*, *101*, 2201–2214, doi:10.1007/s00531-012-0783-2.
Castañares, L. M., and S. Robles (2004), El vulcanismo del Albiense-Santoniense en la Cuenca Vasco-Cantábrica, in *Geología de España*, edited by J. A. Vera, pp. 306–308, SGE-IGME, Madrid.
Choukroune, P. (1992), Tectonic evolution of the Pyrenees, *Annu. Rev. Earth Planet. Sci.*, *20*, 143–158, doi:10.1146/annurev.earth.20.1.143.
Dautria, J. M., J. M. Liotard, D. Bosch, and O. Alard (2010), 160 Ma of sporadic basaltic activity on the Languedoc volcanic line (Southern France): A peculiar case of lithosphere-asthenosphere interplay, *Lithos*, *120*, 202–222, doi:10.1016/j.lithos.2010.04.009.
Dubois, P., and J. C. Seguin (1978), Les flyschs crétacé et éocène de la zone commingeoise et leur environnement, *Bull. Soc. Géol. Fr.*, *20*(5), 657–671, doi:10.2113/gssgfbull.S7-XX.5.657.
Enrique, P. (2009), Las espesartitas, camptonitas y bostonitas del complejo intrusivo de Aiguablava (Cadenas Costeras Catalanas): Cartografía y composición, *Geogaceta*, *47*, 125–128.
Fernández-Mendiola, P. A., and J. García-Mondéjar (2003), Carbonate platform growth influenced by contemporaneous basaltic intrusión (Albian of Larrano, Spain), *Sedimentology*, *50*, 961–978, doi:10.1046/j.1365-3091.2003.00591.x.
Feuillée, P., and P. Rat (1971), Structures et Paléogéographies Pyrénéo-Cantabriques, in *Proceedings Symposium, Historie Structurale du Golfe de Gascogne*, Publ. Inst. Fr. Pét. Collect. Colloq. Sémin., vol. 22, pp. 1–48, Technip, Paris.
Filleaudeau, P. Y., F. Mouthereau, and R. Pik (2012), Thermo-tectonic evolution of the south-central Pyrenees from rifting to orogeny: Insights from detrital zircon U/Pb and (U-Th)/He thermochronometry, *Basin Res.*, *24*, 401–417, doi:10.1111/j.1365-2117.2011.00535.x.
Fitzgerald, P. G., J. A. Muñoz, P. J. Coney, and S. L. Baldwin (1999), Asymmetric exhumation across the Pyrenean orogen: Implications for the tectonic evolution of a collisional orogen, *Earth Planet. Sci. Lett.*, *173*, 157–170, doi:10.1016/S0012-821X(99)00225-3.
Galé, C., and E. Arranz (2001), Volcaniclastic Cretaceous magmatism in the Southern Pyrenees: Preliminary age and source data, Journal of Conference Abstracts EUG XI, 6(1), 577.
Galé, C., M. Lago, and E. Arranz (2000), Petrología del magmatismo alcalino básico del sector de Denuy (Huesca), *Geotemas*, *1*, 245–249.
García-Senz, J. (2002), Cuencas extensivas del Cretácico inferior en los Pirineos centrales, formación y subsecuente inversion, PhD thesis, Univ. Barcelona, Barcelona, Spain.
Garrido-Megías, A., and L. M. Ríos-Aragüés (1972), Síntesis geológica del Secundario y Terciario entre los ríos Cinca y Segre, *Bol. Geol. Min.*, *83*, 1–47.
Gee, J. S., and D. V. Kent (2007), Source of oceanic magnetic anomalies and the geomagnetic polarity timescale, in *The Treatise on Geophysics 5: Geomagnetism*, edited by M. Kono, pp. 455–507, Elsevier, Amsterdam.
Gil-Imaz, A., M. Lago-San José, C. Galé, O. Pueyo-Anchuela, T. Ubide, P. Tierz, and B. Oliva-Urcia (2012), The Permian mafic dyke swarm of the Panticosa pluton (Pyrenean Axial Zone, Spain): Simultaneous emplacement with the late-Variscan extensión, *J. Struct. Geol.*, *42*, 171–183, doi:10.1016/j.jsg.2012.05.008.
Golberg, J. M., H. Maluski, and A. F. Leyreloup (1986), Petrological and age relationship between emplacement of magmatic breccia, alkaline magmatism, and static metamorphism in the North Pyrenean Zone, *Tectonophysics*, *129*, 275–290, doi:10.1016/0040-1951(86)90256-8.
Gong, Z., C. G. Langereis, and T. A. T. Mullender (2008), The rotation of Iberia during the Aptian and the opening of the Bay of Biscay, *Earth Planet. Sci. Lett.*, *273*, 80–93, doi:10.1016/j.epsl.2008.06.016.
Gong, Z., D. J. J. Van Hinsbergen, R. L. M. Vissers, and M. J. Dekkers (2009), Early Cretaceous syn-rotational extension in the Organyà basin—New constraints on the palinspastic position of Iberia during its rotation, *Tectonophysics*, *473*, 312–323, doi:10.1016/j.tecto.2009.03.003.
Henry, P., B. Azambre, R. Montigny, M. Rossy, and R. K. Stevenson (1998), Late mantle evolution of the Pyrenean sub-continental lithospheric mantle in the light of new ^{40}Ar–^{39}Ar and Sm–Nd ages on pyroxenites and peridotites (Pyrenees, France), *Tectonophysics*, *296*, 103–123, doi:10.1016/S0040-1951(98)00139-5.
Ijlst, L. (1973), Laboratory overflow-centrifuge for heavy liquid mineral separation, *Am. Mineral.*, *58*, 1088–1093.
Jammes, S., G. Manatschal, L. Lavier, and E. Masini (2009), Tectonosedimentary evolution related to extreme crustal thinning ahead of a propagating ocean: Example of the western Pyrenees, *Tectonics*, *28*, TC4012, doi:10.1029/2008TC002406.
Jammes, S., L. Lavier, and G. Manatschal (2010), Extreme crustal thinning in the Bay of Biscay and the Western Pyrenees: From observations to modeling, *Geochem. Geophys. Geosyst.*, *11*, Q10016, doi:10.1029/2010GC003218.
Juez-Larré, J., and P. A. M. Andriessen (2002), Post Late Paleozoic tectonism in the southern Catalan Coastal Ranges (NE Spain), assessed by apatite fission track analysis, *Tectonophysics*, *349*, 113–129, doi:10.1016/S0040-1951(02)00049-5.
Juez-Larré, J., and P. A. M. Andriessen (2006), Tectonothermal evolution of the northeastern margin of Iberia since the break-up of Pangea to present, revealed by low-temperature fission-track and (U–Th)/He thermochronology. A case history of the Catalan Coastal Ranges, *Earth Planet. Sci. Lett.*, *243*, 159–180, doi:10.1016/j.epsl.2005.12.026.
Koppers, A. A. P. (2002), ArArCALC-software for ^{40}Ar/^{39}Ar age calculations, *Comput. Geosci.*, *28*, 605–619, doi:10.1016/S0098-3004(01)00095-4.
Koppers, A. A. P., H. Staudigel, and J. R. Wijbrans (2000), Dating crystalline groundmass separates of altered Cretaceous seamount basalts by the ^{40}Ar/^{39}Ar incremental heating technique, *Chem. Geol.*, *166*, 139–158, doi:10.1016/S0009-2541(99)00188-6.
Kuiper, K. F., A. Deino, F. J. Hilgen, W. Krijgsman, P. R. Renne, and J. R. Wijbrans (2008), Synchronizing rock clocks of earth history, *Science*, *320*, 500–504, doi:10.1126/science.1154339.
Lagabrielle, Y., and J. L. Bodinier (2008), Submarine reworking of exhumed subcontinental mantle rocks: Field evidence from the Lherz peridotites, French Pyrenees, *Terra Nova*, *20*, 11–21, doi:10.1111/j.1365-3121.2007.00781.x.

Lagabrielle, Y., P. Labaume, and M. de Saint Blanquat (2010), Mantle exhumation, crustal denudation, and gravity tectonics during Cretaceous rifting in the Pyrenean realm (SW Europe): Insights from the geological setting of the lherzolite bodies, *Tectonics*, *29*, TC4012, doi:10.1029/2009TC002588.

Lago, M., A. Pocovi, J. Bastida, E. Arranz, R. Vaquer, R. Dumitrescu, A. Gil-Imaz, and M. P. Lapuente (1996), El magmatismo alcalino, Hettangiense, en el dominio nor-oriental de la Placa Ibérica, *Cuad. Geol. Ibérica*, *20*, 109–138.

Lavenu, A. P. C., J. Lamarche, A. Gallois, and B. D. M. Gauthier (2013), Tectonic versus diagenetic origin of fractures in a naturally fractured carbonate reservoir analog (Nerthe anticline, southeastern France), *AAPG Bull.*, *97*(12), 2207–2232, doi:10.1306/04041312225.

Leleu, S., J.-F. Ghienne, and G. Manatschal (2009), Alluvial fan development and morpho-tectonic evolution in response to contractional fault reactivation (Late Cretaceous–Palaeocene), Provence, France, *Basin Res.*, *21*(2), 157–187, doi:10.1111/j.1365-2117.2008.00378.x.

López, B. (2013), Extensional salt tectonics in the Cotiella post-rift basin (south-central Pyrenees): 3D structure and evolution, PhD thesis, Univ. Barcelona, Barcelona, Spain.

Losantos, M., J. Montaner, J. Solá, E. Mató, J. M. Sampsó, J. Picart, F. Calvet, P. Enrique, M. Ferrés, and J. Solé (2000), Mapa Geològic de Catalunya 1:25000, Palafrugell, 335-1-1 (79-25), ICC, Servei Geològic de Catalunya.

Losantos, M., C. Roqué, and L. Pallí (2004), Mapa Geològic de Catalunya 1:25000, Calella de Palafrugell, 335-1-2 (76-26), ICC, Servei Geològic de Catalunya.

Matton, G., and M. Jébrak (2009), The Cretaceous Peri-Atlantic Alkaline Pulse (PAAP): Deep mantle plume origin or shallow lithospheric break-up?, *Tectonophysics*, *469*, 1–12, doi:10.1016/j.tecto.2009.01.001.

McClay, K., J. A. Muñoz, and J. García-Senz (2004), Extensional salt tectonics in a contractional orogen: A newly identified tectonic event in the Spanish Pyrenees, *Geology*, *32*, 737–740, doi:10.1130/G20565.1.

McDougall, I., and T. M. Harrison (1999), *Geochronology and Thermochronology by the $^{40}Ar/^{39}Ar$ Method*, Oxford Univ. Press, Oxford.

Mey, P. H. W. (1968), Geology of the Upper Ribargozana and Tor valleys, Central Pyrenees (Spain), *Leidse Geol. Meded.*, *41*, 229–292.

Miranda, R., V. Valadares, P. Terrinha, J. Mata, M. R. Azevedo, M. Gaspar, J. C. Kullberg, and C. Ribeiro (2009), Age constraints on the Late Cretaceous alkaline magmatism on the West Iberian Margin, *Cretaceous Res.*, *30*, 575–586, doi:10.1016/j.cretres.2008.11.002.

Montigny, R., B. Azambre, M. Rossy, and R. Thuizat (1982), Etude K / Ar du magmatisme basique lié au Trias supérieur des Pyrénées. Conséquences méthodologiques et paléogéographiques, *Bull. Mineral.*, *105*, 673–680.

Montigny, R., B. Azambre, M. Rossy, and R. Thuizat (1986), K-Ar study of Cretaceous magmatism and metamorphism in the Pyrenees: Age and length of rotation of the Iberian Peninsula, *Tectonophysics*, *129*, 257–273, doi:10.1016/0040-1951(86)90255-6.

Muñoz, J. A. (1992), Evolution of a continental collision belt: ECORS-Pyrenees crustal balanced cross-section, in *Thrust Tectonics*, edited by K. R. McClay, pp. 235–246, Chapman & Hall, London.

Neres, N., J. M. Miranda, and E. Font (2013), Testing Iberian kinematics at Jurassic-Cretaceous times, *Tectonics*, *32*, 1312–1319, doi:10.1002/tect.20074.

O'Connor, J. M., P. Stoffers, J. R. Wijbrans, and T. J. Worthington (2007), Migration of widespread long-lived volcanism across the Galápagos Volcanic Province: Evidence for a broad hotspot melting anomaly?, *Earth Planet. Sci. Lett.*, *263*, 339–354, doi:10.1016/j.epsl.2007.09.007.

Oliva-Urcia, B., A. M. Casas, R. Soto, J. J. Villalaín, and K. Kodama (2011), A transtensional basin model for the Organyà basin (central southern Pyrenees) based on magnetic fabric and brittle structures, *Geophys. J. Int.*, *184*, 111–130, doi:10.1111/j.1365-246X.2010.04865.x.

Olivet, J. L. (1996), La cinématique de la plaque Ibérique, *Bull. Centres Rech. Explor.-Prod. Elf-Aquitaine*, *20*, 131–195.

Pallí, L., C. Roqué, and I. Capellá (1993), Mapa Geològic de Sta. Coloma de Farners 1:10.000, Universitat de Girona.

Pirajno, F. (2010), Intracontinental strike-slip faults, associated magmatism, mineral systems and mantle dynamics: Examples from NW China and Altay-Sayan (Siberia), *J. Geodyn.*, *50*(3–4), 325–346, doi:10.1016/j.jog.2010.01.018.

Poujol, M., P. Boulvais, and J. Kosler (2010), Regional-scale Cretaceous albitization in the Pyrenees: Evidence from in situ U–Th–Pb dating of monazite, titanite and zircon, *J. Geol. Soc. London*, *167*, 751–767, doi:10.1144/0016-76492009-144.

Puigdefàbregas, C., and P. Souquet (1986), Tecto-sedimentary cycles and depositional sequences of the Mesozoic and Tertiary from the Pyrenees, *Tectonophysics*, *129*, 173–203, doi:10.1016/0040-1951(86)90251-9.

Renne, P. R., et al. (2009), Data reporting norms for $^{40}Ar/^{39}Ar$ geochronology, *Quat. Geochronol.*, *4*, 346–352, doi:10.1016/j.quageo.2009.06.005.

Rock, N. M. S. (1982), The Late Cretaceous Alkaline Igneous Province in the Iberian Peninsula, and its tectonic significance, *Lithos*, *15*, 111–131, doi:10.1016/0024-4937(82)90004-4.

Rosenbaum, G., G. S. Lister, and C. Duboz (2002), Relative motions of Africa, Iberia and Europe during Alpine orogeny, *Tectonophysics*, *359*, 117–129, doi:10.1016/S0040-1951(02)00442-0.

Rossi, P., A. Cocherie, C. M. Fanning, and Y. Ternet (2003), Datation U–Pb sur zircons des dolérites tholéiitiques pyrénéennes (ophites) à la limite Trias–Jurassique et relations avec les tufs volcaniques dits « infra-liasiques » nord-pyrénéens, *C. R. Geosci.*, *335*, 1071–1080, doi:10.1016/j.crte.2003.09.01.

Rossy, M., B. Azambre, and F. Albarède (1992), REE and Sr-Nd isotope geochemistry of the alkaline magmatism from the Cretaceous North-Pyrenean Rift Zone (France-Spain), *Chem. Geol.*, *97*(1–2), 33–46, doi:10.1016/0009-2541(92)90134-Q.

Sanz, T., M. Lago, A. Gil, C. Galé, J. Ramajo, T. Ubide, A. Pocoví, P. Tierz, and P. Larrea (2013), The Upper Triassic alkaline magmatism in the NW Iberian Chain (Spain), *J. Iber. Geol.*, *39*(2), 203–222, doi:10.5209/rev_JIGE.2013.v39.n1.41759.

Scarrow, J. H., F. Bea, P. Montero, J. F. Molina, and A. P. M. Vaughan (2006), A precise late Permian $^{40}Ar/^{39}Ar$ age for Central Iberian camptonitic lamprophyres, *Geol. Acta*, *4*(4), 451–459, doi:10.1344/105.000000346.

Scarrow, J. H., J. F. Molina, F. Bea, P. Montero, and A. P. M. Vaughan (2011), Lamprophyre dikes as tectonic markers of late orogenic transtension timing and kinematics: A case study from the Central Iberian Zone, *Tectonics*, *30*, TC4007, doi:10.1029/2010TC002755.

Schärer, U., P. de Parseval, M. Polvé, and M. de Saint Blanquat (1999), Formation of the Trimouns talc-chlorite deposit (Pyrenees) from persistent hydrothermal activity between 112 and 97 Ma, *Terra Nova*, *11*, 30–37, doi:10.1046/j.1365-3121.1999.00224.x.

Schoeffler, J., J. Henry, and J. Villanova (1964), État des travaux de cartographie géologique réalisés par la Société nationale des pétroles d'Aquitaine (SNPA) dans les Pyrénées occidentals, *C. R. Somm. Soc. Géol. Fr.*, *7*, 241–246.

Sibuet, J. C., S. P. Srivastava, and W. Spakman (2004), Pyrenean orogeny and plate kinematics, *J. Geophys. Res.*, *109*, B08104, doi:10.1029/2003JB002514.

Solé, J., M. Delaloye, and P. Enrique (1998), K-Ar ages in biotites and K-feldspars from the Catalan Coastal Batholith: Evidence of a post-Hercynian overprinting, *Eclogae Geol. Helv.*, *91*, 139–148, doi:10.5169/seals-168413.

Solé, J., T. Pi, and P. Enrique (2003), New geochronological data on the late Cretaceous alkaline magmatism of the northeast Iberian Peninsula, *Cretaceous Res.*, *24*, 135–140, doi:10.1016/S0195-6671(03)00030-2.

Srivastava, S. P., J. C. Sibuet, S. Cande, W. D. Roest, and I. D. Reid (2000), Magnetic evidence for slow seafloor spreading during the formation of the Newfoundland and Iberian margins, *Earth Planet. Sci. Lett.*, *182*, 61–76, doi:10.1016/S0012-821X(00)00231-4.

Steiger, R. H., and E. Jäger (1977), Subcommission on geochronology—Convention on use of decay constants in geochronology and cosmochronology, *Earth Planet. Sci. Lett.*, *36*, 359–362, doi:10.1016/0012-821X(77)90060-7.
Ubide, T., M. Lago, E. Arranz, C. Galé, and P. Larrea (2010a), The lamprophyric sub-vertical dyke swarm from Aiguablava (Catalonian Coastal Ranges): Petrology and composition, *Geogaceta*, *49*, 83–86.
Ubide, T., R. Van Elsas, J. R. Wijbrans, E. Arranz, M. Lago, C. Galé, and P. Larrea (2010b), A visual method for separating amphibole (kaersutite) and Mg-clinopyroxene, *Macla*, *13*, 217–218.
Ubide, T., C. Galé, E. Arranz, M. Lago, Z. França, P. Larrea, and P. Tierz (2011), Subduction-related signature in late-Variscan lamprophyres from the Catalonian Coastal Ranges (northeast Spain), Abstract Proceedings of the XXV IUGG General Assembly (Melbourne), 1924.
Ubide, T., E. Arranz, M. Lago, C. Galé, and P. Larrea (2012a), The influence of crystal settling on the compositional zoning of a thin lamprophyre sill: A multi-method approach, *Lithos*, *132-133*, 37–49, doi:10.1016/j.lithos.2011.11.012.
Ubide, T., C. Galé, E. Arranz, M. Lago, P. Larrea, P. Tierz, and T. Sanz (2012b), Enriched mantle source for the Cretaceous alkaline lamprophyres from the Catalonian Coastal Ranges (NE Spain), *Mineral. Mag.*, *76*(6), 2475.
Ubide, T., C. Galé, E. Arranz, M. Lago, and P. Larrea (2014), Clinopyroxene and amphibole crystal populations in a lamprophyre sill from the Catalonian Coastal Ranges (NE Spain): A record of magma history and a window to mineral-melt partitioning, *Lithos*, *184–187*, 225–242, doi:10.1016/j.lithos.2013.10.029.
Van der Voo, R. (1969), Paleomagnetic evidence for the rotation of the Iberian Peninsula, *Tectonophysics*, *7*, 5–56, doi:10.1016/0040-1951(69)90063-8.
Velde, D., and J. Tournon (1970), La camptonite de San Feliu de Buxalleu (Province de Gérone, Espagne), *Bull. Soc. Fr. Minér. Cristallogr.*, *93*, 482–487.
Vergés, J., M. Fernández, and A. Martínez (2002), The Pyrenean orogen: Pre-, syn-, and postcollisional evolution, *J. Virtual Explor.*, *8*, 57–76, doi:10.3809/jvirtex.2002.00058.
Vissers, R. L. M., and P. T. Meijer (2012a), Mesozoic rotation of Iberia: Subduction in the Pyrenees?, *Earth Sci. Rev.*, *110*, 93–110, doi:10.1016/j.earscirev.2011.11.001.
Vissers, R. L. M., and P. T. Meijer (2012b), Iberian plate kinematics and Alpine collision in the Pyrenees, *Earth Sci. Rev.*, *114*, 61–83, doi:10.1016/j.earscirev.2012.05.001.
Vitrac-Michard, A., F. Albarède, and B. Azambre (1977), Age Rb-Sr et ^{39}Ar-^{40}Ar de la syénite néphélinique de Fitou (Corbières orientales), *Bull. Soc. Fr. Minéral. Cristallogr.*, *100*, 251–254.
Walker, J. D., and J. W. Geissman, (compilers) (2009), *Geologic Time Scale*, Geol. Soc. of Am., Boulder, Colo., doi:10.1130/2009.CTS004R2C.
Whitchurch, A. L., A. Carter, H. D. Sinclair, R. A. Duller, A. C. Whittaker, and P. A. Allen (2011), Sediment routing system evolution within a diachronously uplifting orogen: Insights from detrital zircon thermochronological analyses from the south-central Pyrenees, *Am. J. Sci.*, *311*, 442–482, doi:10.2475/05.2011.03.
Whitney, D. L., and B. W. Evans (2010), Abbreviations for names of rock-forming minerals, *Am. Mineral.*, *95*, 185–187, doi:10.2138/am.2010.3371.
Wijbrans, J., K. Németh, U. Martin, and K. Balogh (2007), ^{40}Ar/^{39}Ar geochronology of Neogene phreatomagmatic volcanism in the western Pannonian Basin, Hungary, *J. Volcanol. Geotherm. Res.*, *164*, 193–204, doi:10.1016/j.jvolgeores.2007.05.009.
Wilson, M. (1989), *Igneous Petrogenesis, A Global Tectonic Approach*, Springer, London.
Ziegler, P. A., and S. Cloetingh (2004), Dynamic processes controlling evolution of rifted basins, *Earth Sci. Rev.*, *64*, 1–50, doi:10.1016/S0012-8252(03)00041-2.